

Portrayal of Complex Dynamic Properties of Sugarcane Defensin 5 by NMR: Multiple Motions Associated with Membrane Interaction

Viviane Silva de Paula,¹ Guilherme Razzera,¹ Eliana Barreto-Bergter,² Fabio C.L. Almeida,¹ and Ana Paula Valente^{1,*}

¹Centro Nacional de Ressonância Magnética Nuclear de Macromoléculas, Instituto de Bioquímica Médica, Rio de Janeiro, RJ 21941-902, Brazil

²Instituto de Microbiologia, Universidade Federal do Rio de Janeiro, Rio de Janeiro, RJ 21941-902, Brazil

*Correspondence: valente@cnrmn.bioqmed.ufrj.br

DOI 10.1016/j.str.2010.11.011

SUMMARY

Defensins are essentially ancient natural antibiotics with potent activity extending from lower organisms to humans. Sd5 is a recently described antifungal defensin that appears to be the result of a recent gain of function. We reported here the solution NMR structure of Sd5 and characterized the backbone dynamics in the free state and in the presence of membrane models. ¹⁵N relaxation dispersion measurements indicate intrinsic conformational exchange processes, showing two clear distinct k_{ex} , 490 and 1800 s⁻¹. These multiple motions may be related to transient twisting or breathing of the α helix and β sheet. The stages of membrane recognition and disruption by Sd5 over a large timescale range were mapped and demonstrated that Sd5 in solution sampled an ensemble of different conformations, of which a subset is selected upon membrane binding. Defensins share similar structures, but we demonstrated here that their dynamics can be extremely diverse.

INTRODUCTION

Several studies have shown that proteins do not exist as a single structure in solution but fluctuate among an ensemble of conformations and that these dynamic properties are essential for biological function (Tsai et al., 1999; Lee et al., 2000; Henzler-Wildman et al., 2007; Mittermaier and Kay, 2009). This represents the balance between the tendency to find the lowest energy level and the tendency to populate as many levels as possible for a given thermal energy. The analysis of time- or ensemble-averaged structures does not provide a complete description of protein function and behavior. Such complete understanding requires not only high resolution protein structures, but also information on how these structures change with time (Mittermaier and Kay, 2009; Cavanagh and Akke, 2000).

Discrete conformational states are separated by energy barriers that are related to the kinetics of interconversion

(Henzler-Wildman and Kern, 2007; Boehr, 2009). Proteins interconvert over a broad range of timescales, from picoseconds to nanoseconds for bond oscillations and rotations, to micro to milliseconds for loop and larger domain motions and to seconds to hours for slow motions. NMR spectroscopy is able to probe a broad range of timescales, and different strategies can be used to quantify each type of motion (Meiler et al., 2001).

Important results have been obtained using a relaxation dispersion technique that permits the analysis of conformational exchange on the μ s-ms timescale (Loria et al., 2008; Palmer, 2004; Vallurupalli and Kay, 2006). Kern and co-workers analyzed adenylate kinase, showing that the opening of the nucleotide lid is the rate-limiting step for enzymatic catalysis (Wolf-Watz et al., 2004; Mulder et al., 2001; Volkman et al., 2001). Also, Kay and co-workers analyzed the T4 lysozyme mutant L99A and showed that it interconverts between a ligand-inaccessible conformer and a ligand-accessible state at 2 kcal mol⁻¹ higher free energy, referred to as the excited state. The excited state is characterized by a decrease in the number of stabilizing interactions relative to the ground state, with an increase in entropy consistent with a more dynamic structure (Mulder et al., 2001). Structural details of the excited state have recently been obtained for the allosteric protein NtrC, where transient hydrogen bonds are probably responsible for guiding the conversion between inactive and active conformations (Gardino et al., 2009).

A similar approach has been applied to study protein-protein interactions (Forman-Kay, 1999; Frederick et al., 2007; Valente et al., 2006). For binding interfaces, relaxation data have demonstrated heterogeneous behavior. Certain systems are more dynamic in the free than in the bound state, suggesting that binding restricts the conformations. In other systems, as the binding site becomes more structured, other regions become more dynamic, a phenomenon referred to as entropic compensation. In addition, certain positions on the binding surface can be highly dynamic in both free and bound states (Frederick et al., 2007; Valente et al., 2006). Relaxation measurements have revealed that for membrane interaction events, protein binding sites exhibit conformational diversity equilibria among pre-existing conformations. In the presence of a ligand, one conformation is stabilized, followed by a population shift toward the bound conformation state (Valente et al., 2006).

Our group studies the dynamic properties of defensins and their interactions with membrane models. Some important structural features can be identified by comparing the plant defensins: (1)

defensins contain a high level of diversity in their primary structure despite having the same global fold, which is composed of three antiparallel β strands, one α helix and four disulfide bridges; (2) there is no amino acid signature that enables the assignment of their diverse activity, so their antimicrobial activity cannot be easily predicted; (3) defensins exhibit coevolution of the host-pathogen relationship, where the ability to accommodate mutations is an important tool in avoiding resistance; (4) they are positively charged at physiological pH, and this is related to the initial interaction with the anionic head groups of the microbial membrane lipids; and (5) they have hydrophobic properties that enable interaction of the peptide with the core of the membrane. Recently, new data have shown that membrane damage is only one among several mechanisms involved in the antibiotic action of defensins (Aerts et al., 2008).

In our recent studies of the Psd1 defensin (de Medeiros et al., 2010), we used NMR relaxation methods to characterize the change in dynamic behavior of Psd1 resulting from interaction with membrane models with glucosylceramide extracted from the hyphae of *Fusarium solani* (CMH). Our investigations revealed that Psd1 behaves as a well-structured protein in solution. The conserved Gly12 residue is a flexible hinge in loop1, imposing conformational exchange in its vicinity. This entire region was mapped as the major membrane binding epitope, and its dynamic properties support the idea that conformational selection is the binding mechanism in regions around loop 1 in Psd1.

In this paper, we describe the solution NMR structure and dynamics of Sd5, a recently characterized defensin from *Saccharum officinarum* (De-Paula et al., 2008). Sd5 is the result of a relatively recent gain of function because Sd5 showed similarity only to other defensins in the same tribe, the Andropogoneae. Therefore, it probably evolved less than nine million years ago (De-Paula et al., 2008). Sd5 adopted a typical cysteine-stabilized α/β motif (CS $\alpha\beta$) that is extremely similar to other plant defensins, as expected from the strong conservation of the defensin fold. The major difference is an unstructured C-terminal region. Here, we use Carr-Purcell-Meiboom-Gill (CPMG)-based dispersion experiments (Cornilescu et al., 1999), which are sensitive to millisecond (ms) exchange dynamics between states, to probe the motion of Sd5 in an attempt to address its dynamic properties. ^{15}N relaxation rates revealed that several regions of the protein are dynamic on the ms timescale, with at least two distinct motions that can account for the conformational fluctuations, despite the stabilization by four disulfide bonds.

We also showed the effect of membrane models on the dynamic properties of Sd5. In the early stages of membrane interaction, as mapped using phospholipid vesicles, the binding sites showed increased conformational exchange on the μs -ms timescale, leading to the increase in R_2 values. Amino acids in exchange in the free state remain and contiguous regions start to undergo conformation exchange upon vesicle interaction. In the later stages of membrane insertion, as mapped using DPC micelles, Sd5 was stabilized in several discrete conformations exhibiting slow dynamic exchange. The data presented herein monitored protein dynamic properties through the events of membrane recognition and insertion. Our results contribute to understanding the structural and dynamic requirements associated with defensins membrane interaction and disruption.

RESULTS

Structure Calculation of Sd5

The structure of Sd5 was determined using distance and angle restraints derived by solution NMR methodology. A representative conformer of Sd5 and the final 20 energy-minimized conformers are shown in Figures 1A and 1B (available online). The global fold of Sd5 is the well-known cysteine-stabilized $\alpha\beta$ (CS $\alpha\beta$) motif, which consists of a triple-stranded antiparallel β sheet comprising residues 8–11 (β 1), 38–43 (β 2), and 50–57 (β 3), and one α helix comprising residues 23–33. Moreover, this fold is stabilized by eight disulfide-linked cysteines, with disulfide bonds linking C9–C57, C20–C42, C26–C51, and C30–C53. The loop1 is stabilized by a disulfide bond between Cys20 and Cys42, linking the loop to strand β 2 of the β sheet. The connection between strands β 2 and β 3 is made by a loop (loop2) between residues Gly44 and Lys49.

The first 7 residues from the N terminal region and the last 14 residues from the C-terminal region and loop1 are poorly defined due to intrinsic disorder consistent with the relaxation parameters, as described below. The rest of the Sd5 structure shows high precision, with a root-mean-square deviation of 0.48 Å for the backbone atoms. Details regarding the structure calculation and the parameters defining the quality of the structures are summarized in Table S1 and Figure S1. A PROCHECK-NMR analysis of the structure ensemble gave 83% and 14% of the backbone angles in the most favored regions and additionally allowed regions of the Ramachandran plot, respectively.

The electrostatic potential of the Sd5 surface shows asymmetry in charge distribution and has a highly positive face that includes loops 1 and 2 (Figure 1D). The other side of the molecule, bearing the loop between the α helix and β 2 strand, exhibits both negatively charged and neutral regions.

Dynamic Behavior of Sd5

Analysis of the HSQC spectrum of Sd5 showed that it presents dynamic processes active on the slow, intermediate and fast NMR timescales: some residues from the N- and C-terminal regions appear as a highly intense set of peaks. For instance, Leu66, Trp68 H ϵ 1, and Leu71 undergo slow motions on the chemical shift timescale, as indicated by the fact that they are duplicated in the HSQC spectrum (Figure S2). This peak duplication may be related to *cis/trans* isomerization of the Trp68–Pro69 peptide bond, although we could not find any evidence in the NOESY spectrum of the *cis* conformer (i.e., NOEs $\alpha\text{H}-\alpha\text{H}$ or $\alpha\text{H}-\delta\text{H}$ W68–P69 at a mixing time of 120 ms).

Additionally, other peaks from different regions of Sd5 displayed line broadening, suggesting intermediate motions, on the μs -ms timescale.

To understand the complex dynamics of Sd5, we measured a complete set of backbone amide ^{15}N relaxation rates in the temperature range of 15°C–30°C (Figure 2; Table S2). The R_2 values for several residues in the secondary structures were different than the average, typical of internal motion on μs -ms timescale. This was observed more clearly by analyzing the R_2/R_1 ratio, which is independent of any fitting. Figure 2D shows that the residues Cys9, Lys10, Arg12, Asp25, Ala28, Ala29, Val31, Lys32, Glu33, Ser34, Gly44, Lys49, Gln50, Cys51, Thr54, and Lys55 present R_2/R_1 values greater than the average in agreement with

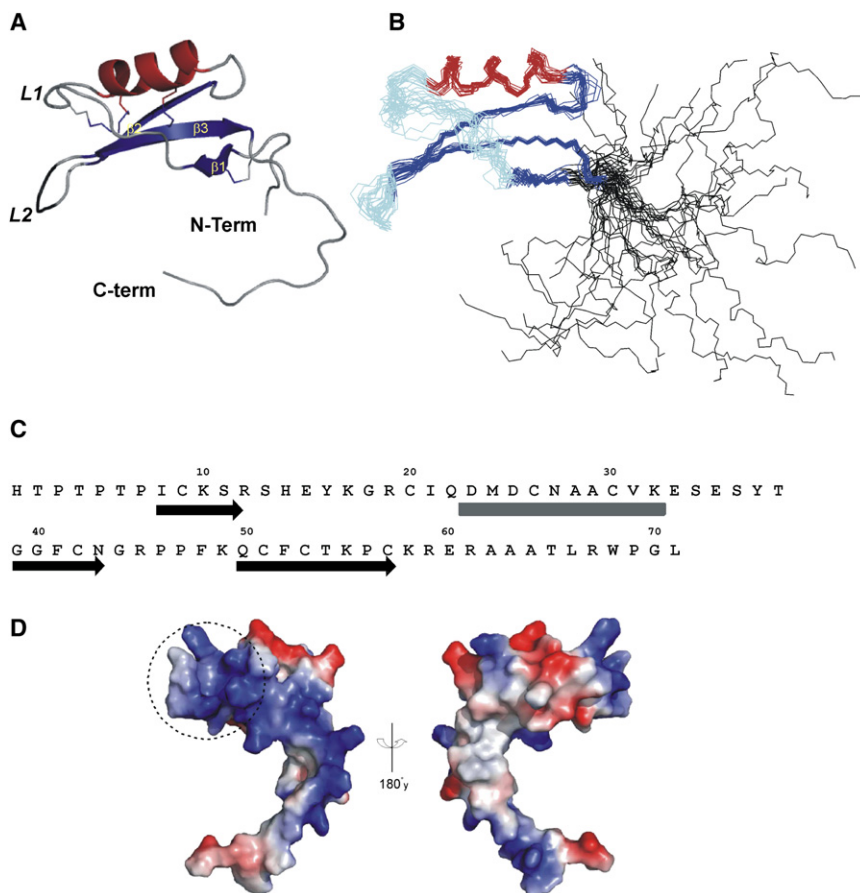


Figure 1. NMR Solution Structure of Sugar-cane Defensin 5, Sd5

(A) The ribbon representation. Helix is colored in red and strands in blue. The *cis* Pro-Pro-Phe sequence motif located on loop 2 is highlighted in black.

(B) Ensemble of 20 refined conformers overlaid with the backbone atoms of the secondary structure residues Ile8-Cys57.

(C) Secondary structure elements in Sd5. Arrows represent the β strands and rectangle the helix.

(D) The charge distribution on the Sd5 surface. Positively charged electrostatic potential is colored blue, and negatively charged electrostatic potential is colored red. The two images are related by a 180° rotation around the y axis. The positively charged loop 1 is circled. Structure figures and electrostatic potential were produced using PyMol (DeLano, 2002) (PDB accession code: 2KSK).

See also Figures S1 and S2.

the suggestion of conformational exchange. The exchange process for these regions increased to fast-intermediate motions with temperature. In addition, the resonance line shapes for Lys17, Asp23, Glu35, Asn43, and Phe52 showed extensive broadening, due to intermediate exchange at all temperatures, hampering the measurements. All of these features indicated that Sd5 is characterized in solution by a distribution of conformations. In particular, this exchange can be observed in the α helix and β sheet regions.

The extended model-free formalism of Lipari-Szabo was used to analyze the ^{15}N relaxation data using the program Tensor2 (Dosset et al., 2000). A correlation time for protein tumbling (τ_c) of 5.1 ns at 25°C was estimated from the R_2/R_1 ratio excluding those residues exhibiting below-average ^{15}N , ^1H -NOEs values (<0.65) and those experiencing conformational exchange processes. Thus, the 5.1 ns correlation time is slightly higher than expected for an 8 kDa protein. The C-terminal flexible tail probably contributes to the anisotropic tumbling of the protein, increasing the measured τ_c . Sd5 was confirmed to exist in the monomeric state by gel filtration chromatography. The relaxation rates recorded at 0.2 mM protein or pH 6.0 showed the same results, indicating that the concentration and pH did not affect the R_1 , R_2 and ^{15}N - ^1H NOE values nor the values of S^2 and τ_c (Figure S3). Because the exchange is independent of pH, we concluded that we were not monitoring labile protons exchange.

Using the Lipari-Szabo model-free formalism, we were able to obtain the general order parameter, S^2 , and R_{ex} terms describing the backbone internal motions on fast (nanosecond to picosecond) and slow (millisecond to microsecond) timescales (Figure S4). The N and C termini and loop 1 of Sd5 are highly flexible, presenting S^2 values well below 0.7. Nevertheless, loop 2 of Sd5 has S^2 values 0.79 at 15°C, 0.67 at 25°C, and 0.65 at 30°C, very similar to the average values of the secondary structure elements (0.79 at 15°C and 0.8 at 25°C and 30°C). Thus, loop 2 did not show significant thermal fluctuations, and exhibited a low degree of internal mobility. Asp25, Ala28, Ala29, Val31, Lys32, Gly44, Lys49, and Cys51 of Sd5 showed significant R_{ex} contributions (>3.0 Hz).

To quantify these R_{ex} contributions, we used ^{15}N Carr-Purcell-Meiboom-Gill (CPMG) relaxation dispersion experiments. As expected from the Lipari-Szabo analysis, the dynamical hotspots were widely distributed throughout the protein. Seventeen of the 60 well-resolved correlations in the ^{15}N , ^1H HSQC spectrum showed dispersions with measurable R_{ex} contributions. Figure 3 shows the relaxation dispersion profiles for Ser11, Lys17, Asp25, Ala28, Val31, Asn43, Lys49, and Phe52 recorded at magnetic field strengths of 14.1 and 18.8 T (600 and 800 MHz) at 25°C. The effective decay rate constant of magnetization (R_2^{eff}) decreased as a function of the number of the refocusing pulses (proportional to ν_{CPMG}), indicating that the processes measured are on the ms timescale, where their effects are attenuated by the application of radio frequency pulses (Palmer, 2004). The amplitude of the dispersion curve (an indicator of total R_{ex}) was larger for those residues located at the α helix and $\beta 1$ and $\beta 3$ strands. This is consistent with the ^{15}N relaxation data and model-free analysis described above. Quantitative analysis revealed that the residues in Sd5 could be fitted into two groups: group I ($k_{\text{ex}} = 490 \pm 100 \text{ s}^{-1}$) and group II ($k_{\text{ex}} = 1,800 \pm 440 \text{ s}^{-1}$).

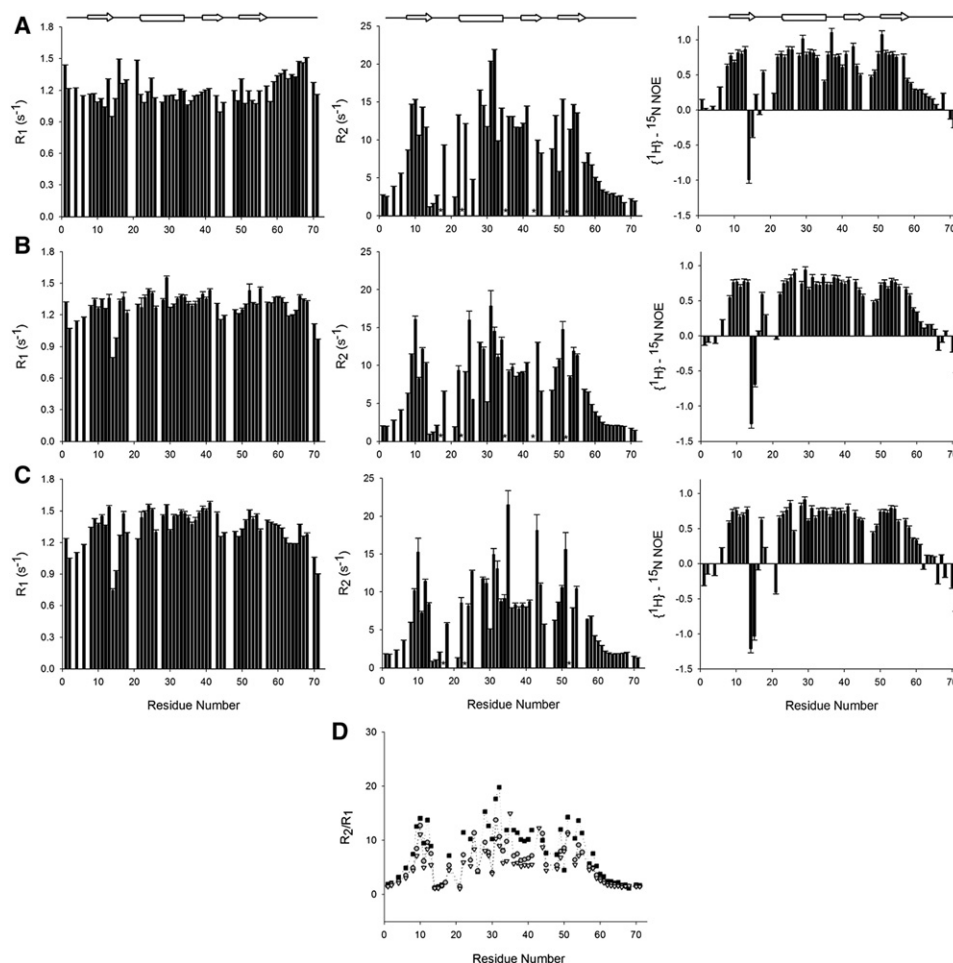


Figure 2. Backbone Dynamics of Sd5

(A–D) Backbone ^{15}N relaxation parameters and heteronuclear $^1\text{H}-^{15}\text{N}$ NOEs for Sd5 at 15°C (A), 25°C (B), and 30°C (C) at 800 MHz plotted as a function of the residue number of Sd5. The experiments were carried out using 5 mM sodium phosphate buffer (pH 4.0), 5 mM sodium azide and 0.6 mM of Sd5. The absence of bars indicates that the values could not be accurately measured due to overlaps or are prolines. The stars indicates the residues where R_2 values could not be measured due broadening of the line beyond detection. (D) ^{15}N R_2 over R_1 ratios (R_2/R_1) of Sd5 at 15°C (black squares), 25°C (gray circles), and 30°C (open triangles).

The errors in the peak intensities were calculated from the two duplicate experiments. See also [Figures S3 and S4](#) and [Table S2](#).

In the majority of cases, the data fit well, and both groups had an average reduced χ^2 value of 1.2 ± 0.9 . In some cases, larger χ^2 values were obtained when the amplitude of the dispersion profile was flatter. These data suggest that two exchange regimes exist at different sites in Sd5. This behavior has not been reported for any other defensin. It is worth mentioning that several technical and experimental improvements in the NMR field during recent years, allowed precise quantitative dynamic studies. Therefore, we are able to probe the dynamic features related to protein function in more detail than hitherto possible.

Mapping the Membrane Binding Site on Sd5

Phospholipid vesicles are kinetically stable, and have small curvature and high lipid packing, as a consequence of that proteins have limited access to their hydrophobic core when compared to micelles ([Leng et al., 2003](#)). Therefore, we used

vesicles to monitor the first events in membrane recognition. Micelles on the other hand, are dynamic entities that are kinetically unstable, with large curvature and tighter packing. Hydrophobic exposure is higher in micelles permitting more direct protein interaction. Summarizing, experiments with vesicles are informative of the initial events of interaction (membrane recognition), whereas experiments with micelles are more likely to yield information on later events, such as membrane insertion and disruption.

To investigate which residues play a role in Sd5 membrane recognition, we recorded a series of $^{15}\text{N}, ^1\text{H}$ HSQC spectra of Sd5 containing DPC micelles or PC:CMH vesicles.

We probed the interaction between Sd5 and PC or PC:CMH vesicles ([Figure 4](#)). The presence of single sharp Sd5 resonances indicated that the binding equilibrium is shifted toward the free state and that the process occurs in the fast exchange regime in the presence of vesicles. No decrease in resonance intensity

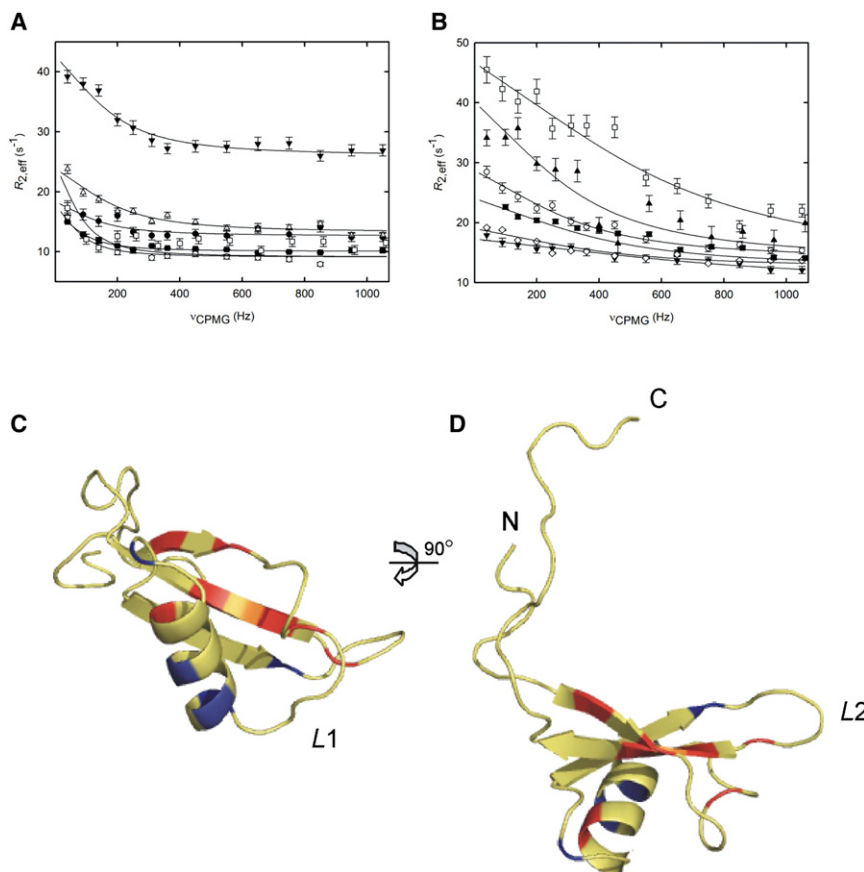


Figure 3. Quantitative Analysis of Exchange Dynamics in Sd5

¹⁵N NMR relaxation dispersion curves were measured at 800 and 600 MHz. Residues in Sd5 had to be fitted in two groups with $k_{ex} = 490 \pm 100$ s⁻¹ for group I (A) and $k_{ex} = 1,800 \pm 440$ s⁻¹ (means \pm SD) for group II (B). Representative residues are shown: Ser11 at 600 MHz (\circ) and 800 MHz (\square), Val31 at 600 MHz (Δ), Lys49 at 600 MHz (\blacksquare), Lys17 at 600 MHz (\blacktriangledown), and Cys9 at 600 MHz (\bullet) for group I; Phe52 at 600 MHz (\square), Asn43 at 600 MHz (\bullet) and 800 MHz (\blacktriangle), Ala28 at 600 MHz (\diamond) and 800 MHz (\blacksquare), Asp25 at 600 MHz (\blacktriangledown) for group II. (C and D) Amides undergoing chemical exchange in Sd5 are colored in red and blue for group I and II, respectively, shown in two views differing by a 90° horizontal rotation. For each relaxation dispersion curve, three triplicate points were collected and used to estimate the absolute uncertainties.

was observed that would be indicative of strong vesicles binding. Nevertheless, we found that the NMR resonances corresponding to Gly70 and Leu71 show slight chemical shift perturbation after the addition of PC alone (0.5 molar equivalents). Interestingly, when we added PC:CMH vesicles (0.5:0.11 molar equivalents) in the ¹⁵N labeled Sd5 sample, the cross-peaks of Gly70 and Leu71 and other cross-peaks showed a significant increase in chemical shift perturbation (Figure 4A). The regions perturbed by the PC:CMH vesicles clustered mainly at loop1, a part of the α helix region (Asp23, Val31, and Lys32), the C-terminal region (Glu60, Gly70, and Leu71) and in the turn between the α helix and β 2 (Ser34, Glu35, Ser36, and Tyr37) (Figures 4B and 4C).

Although PC comprises the vast majority of the PC:CMH vesicle surface (~76%), all of the chemical shift perturbations, except Gly70 and Leu71, were observed only in the presence of CMH. This result lends strong support for the suggestion that the glucosylceramide present in fungal membranes is an important binding receptor for Sd5 binding and other plant defensins (Thevisen et al., 2004).

We observed much more pronounced chemical shift changes in the presence of DPC micelles (Figures 4D–4F). The HSQC spectrum changed continuously with DPC concentration. At 300 mM DPC, the resonances of Sd5 became very broad while maintaining chemical shift dispersion. This behavior hampered the assignment and the relaxation measurements at 300 mM

follows: Tyr16, Lys17, Gly18 and Ile21 from loop 1, Arg45, Phe48, and Lys49 from loop 2 and Ala63, Ala64, Leu66, Trp68, Gly70, and Leu71 from the C-terminal (Figure 4F). Notably, a number of residues that showed substantial changes in chemical shift were solvent-exposed hydrophobic residues or positive charged residues (Figure 1D). This indicated that hydrophobic and Coulombic interactions are important for the interaction of Sd5 with DPC micelles.

Interestingly, at 60 mM, the HSQC spectrum DPC showed that several resonances split into multiple peaks, suggesting the stabilization of multiple conformations (Figures 4D and 4E). For instance, Trp68H_z, which appeared duplicated in the free state, appeared as four peaks in DPC micelles and Lys17 that appeared as a single peak in solution, yielded six resonances in DPC, as did Asp23, Glu35, Lys49, Ala62, Gly70 and Leu71. Remarkably, except for Gly 70 and Leu 71, all residues exhibited conformational exchange in the free state. This result suggests that insertion of Sd5 in the hydrophobic core of the DPC micelle stabilizes several different conformations that interconvert in the slow-intermediate exchange regime.

PC:CMH and DPC Interacting Sites

Altogether the chemical shift perturbation data presented in Figure 4 showed that two distinct region are important for membrane and CMH interaction: the first region, named unspecific, comprised residues that change both in the presence of

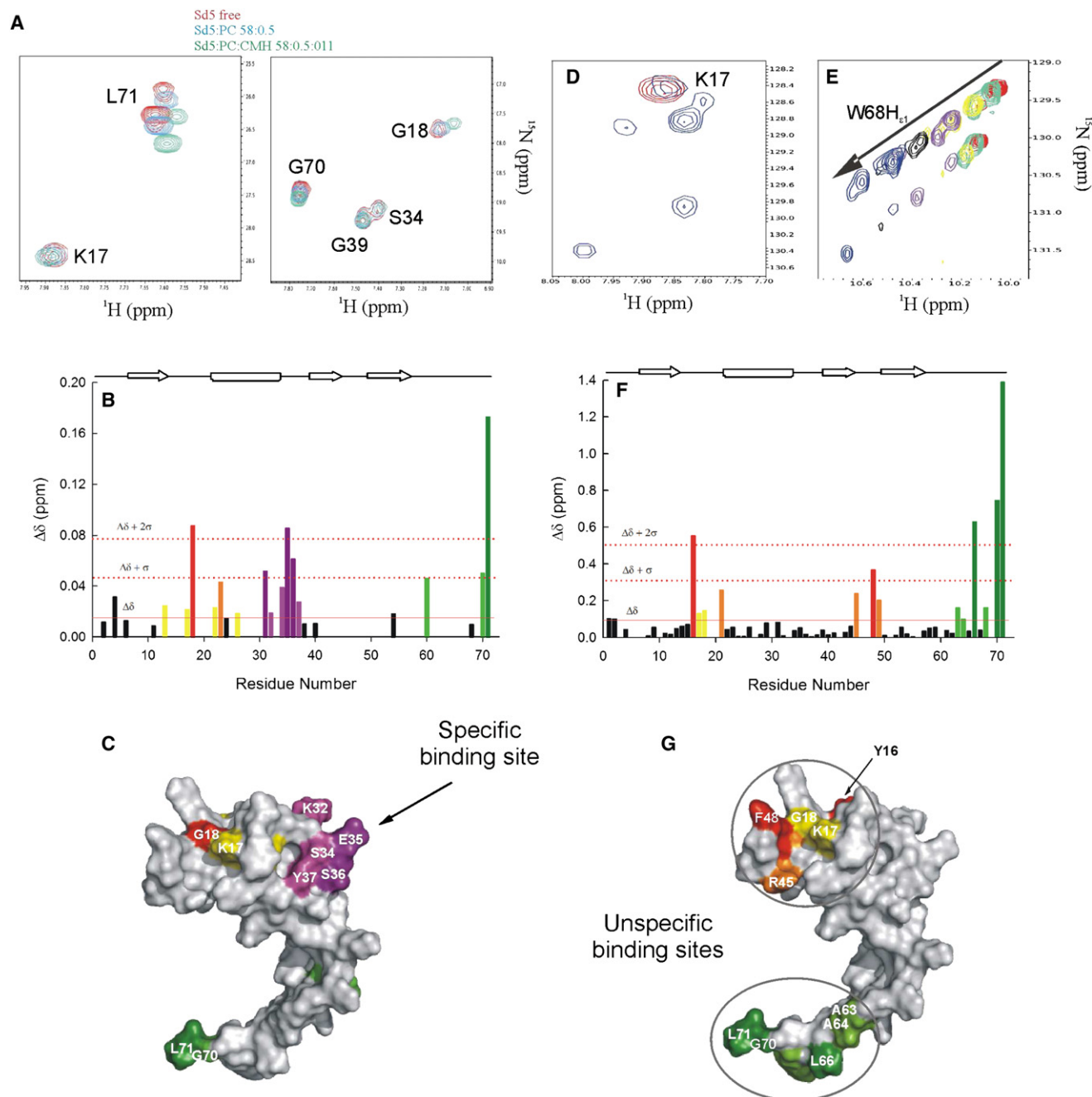


Figure 4. Structural Features of the Sd5 Interaction Surface with Membrane Models

(A, D, and E) Superposition of ^{15}N HSQCs obtained for 0.2 mM Sd5 free in solution (red) and in the presence of membrane models. (A) Chemical shifts changes observed in NMR experiments of Sd5 with PC (in blue) and PC:CMH vesicles (green). (D) Lys17 resonances at 60 mM DPC concentration, showing the presence of multiple conformers (blue). (E) Trp68H ϵ_1 region of the spectrum at 0 (red), 5 (green), 10 (yellow), 15 (purple), 30 (black), and 60 (blue) mM DPC concentrations. (B and F) Chemical shift perturbation as a function of residue number, obtained in the presence of presence of PC:CMH (9:1) vesicles and 60 mM DPC, respectively. The statistical significance of the change seen for an individual residue can be judged by the red horizontal lines.

(C and G) Surface representation of Sd5 with residues affected by the interactions with PC:CMH vesicles and DPC micelles. Defensin domain is colored yellow to purple, and the C-terminal region is colored in green. The unspecific region is circled, and the specific site is colored in purple.

See also Figures S5–S7.

PC:CMH and DPC (residues Arg12, Tyr16, Lys17, Gly18, Ile21, Asp23, Cys26, Arg45, Phe48, Lys49, Ala63, Ala64, Leu66, Trp68, Gly70, and Leu71). We believe that these residues are

responsible for unspecific membrane interaction; the second interacting region enclose residues that only changed in the presence of CMH (purple, residues Val31, Lys32, Ser34, Glu35,

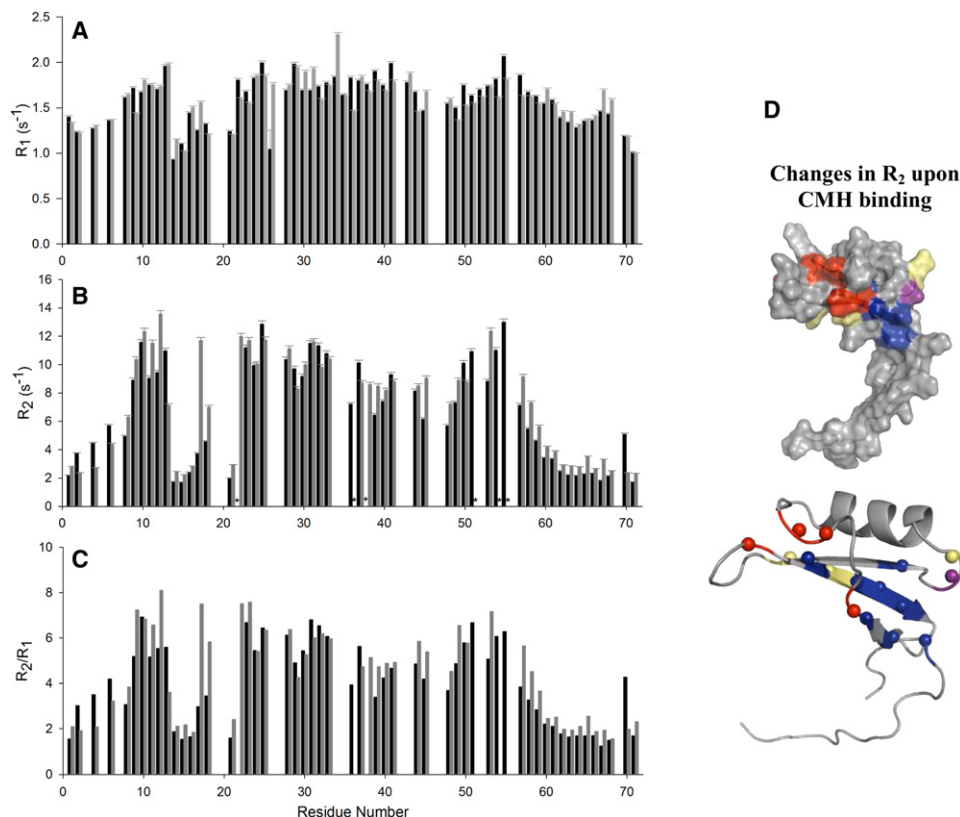


Figure 5. Dynamics in Sd5 during Interaction with PC:CMH Vesicle

Backbone amide relaxation parameters ^{15}N R_1 (A), ^{15}N R_2 (B), and R_1/R_2 ratio (C) as a function of amino acid sequence were recorded at 25°C for Sd5 alone (black bars) and in the presence of PC:CMH (9:1) (gray bars). The absence of bars indicates that the values could not be accurately measured due to overlaps or are prolines. (D) The backbone nitrogen atoms of residues displaying R_2 increased upon interaction with PC:CMH vesicles are shown as colored spheres (specific binding site, purple; unspecific binding site, red; group I residues, blue; missing residues of both Sd5 in its free state and in the presence of vesicles are largely due to significant exchange broadening, light yellow). The errors in the peak intensities were calculated from the two duplicate experiments.

Ser36, and Tyr37) and probably respond for the specific interaction with the membrane target, and was named specific region.

Important to mention that, in the free state, the unspecific interaction region undergoes dynamics in the ps-ns time scale (flexible) while the specific interaction region undergoes exchange in the μs -ms timescale. This association with dynamics could be an important indication of the prime features in Sd5 membrane interaction. We decided then to study the changes in dynamics in the presence of PC:CMH or DPC.

Dynamics Associated with Membrane Binding PC and PC:CMH Vesicles

Although the binding equilibrium was shifted to the free-state, the dynamic changes induced by PC:CMH in Sd5 were revealing. Figures 5A–5C shows the comparison of relaxation parameters. The data showed an increase in R_2 values for residues that belong to the interacting and contiguous regions. Figure 5D shows in Sd5 structure the residues with important increase in R_2 both in the unspecific (in red, residues Arg12, Lys17, Gly18, and Lys49) and specific interaction region (in purple, residue Ser36). We also colored residues located close to the specific interacting region including residues Cys9, Ser11, 51, Cys53, Cys57 were already in exchange in the free

state and increase R_2 values upon interaction. Residues in yellow are the ones in conformational exchange in the free state that remain unchanged in the bound state.

Contrarily, the R_2 values for residues Ser13, Gly70, and residues in the N-terminal region were slightly decreased and residues Gln22 and Thr38, which were broadened in the free state, appear as sharp peaks in the presence of PC:CMH.

The average R_2/R_1 for the Sd5-PC:CMH sample excluding residues located in loop1 and the N and C termini was 6.0, only slightly higher than the value of 5.4 for the protein alone. This result corroborates the idea of small Sd5 insertion in the vesicles. The R_1 values and the heteronuclear NOEs changed slightly in the presence of PC:CMH suggesting that the thermal dynamics did not change significantly on the ps-ns timescale. These results suggest a specific interaction of Sd5 with vesicles containing CMH that leads to an increase in the conformational exchange processes.

DPC Micelles

Only slight difference was observed in either R_1 or the heteronuclear NOE values in the presence of DPC micelles (60 mM). However, R_2 values increased globally. Figure S5 (right panel) shows the increase in R_2/R_1 ratio that was observed for most

of the residues of Sd5. This global change in dynamics resulted from the greater impact of the equilibrium between the free and bound conformations, over the intrinsic conformational process. Therefore, we could not investigate any changes on the μs -ms timescale.

The average R_2/R_1 values for Sd5 were 5.3 and 7.6 when free in solution and micelle bound, respectively (excluding residues in flexible regions). The great elevation of the R_2/R_1 ratio may be explained by complex formation (between Sd5 and the micelles). The calculations assuming anisotropic tumbling yielded a global correlation time of 5.1 ns for free and 7.7 ns for micelle-bound Sd5, again corroborating the idea of greater Sd5 micelle insertion.

We exhaustively attempted to analyze the DPC data based on the Lipari-Szabo model free formalism. Tensor 2 could not fit the data satisfactorily using either the isotropic or anisotropic hydrodynamic model, probably because there is a strong contribution from the exchange between the free and bound states.

Sd5-Induced Leakage of ANTS/DPX from Vesicles Prepared with CMH

The results presented above demonstrated that Sd5 is able to interact with vesicles containing mainly CMH. Also, the complex dynamic behavior of its structure matches the membrane binding site, suggesting an important role in the mechanism of action of Sd5. Membrane insertion increased the conformational dynamics of the binding region, and this may be related to Sd5 membrane disruption. We decided to pursue this hypothesis of membrane disruption using fluorescent probes and different types of vesicles. Leakage of large unilamellar vesicles (LUVs) was examined using the dye/quencher pair ANTS/DPX (Ladokhin et al., 1997; Takeuchi et al., 2004). The total leakage percentage from LUVs consisting of various lipid compositions is plotted as a function of Sd5 concentration in Figure 6 and Table S3. No effect was observed when the vesicles were prepared with PC:PE or PC:PG up to 100 μM Sd5. But when LUVs were prepared with PC:CMH and membrane total lipids of *F. solani*, Sd5 was able to promote vesicle leakage. These data demonstrated that Sd5 is capable of efficiently permeabilizing fungal lipid membranes. Requenched analysis (Ladokhin et al., 1997) showed that the leakage occurred by a graded mechanism in which all vesicles released some of their contents during the active period, rather than by an all-or-none process in which some of the vesicles release all of their contents.

Taken together, these observations reveal that the surface charge of the lipid membrane was not a critical factor in the lipid perturbation activity of Sd5, and the presence of CMH in lipid membranes considerably increased the lipid perturbation activity of Sd5.

DISCUSSION

Antimicrobial peptides that bind to and permeabilize cell membranes are important in innate immunity and defense. They are constantly evolved in nature to overcome continuous microbial adaptation. Defensins are basic, cysteine-rich antimicrobial peptides that accomplish an important role in the innate immunity of their host by combating pathogenic invading microorganisms. They share low primary sequence similarity despite having the same global fold. This is probably due to their having

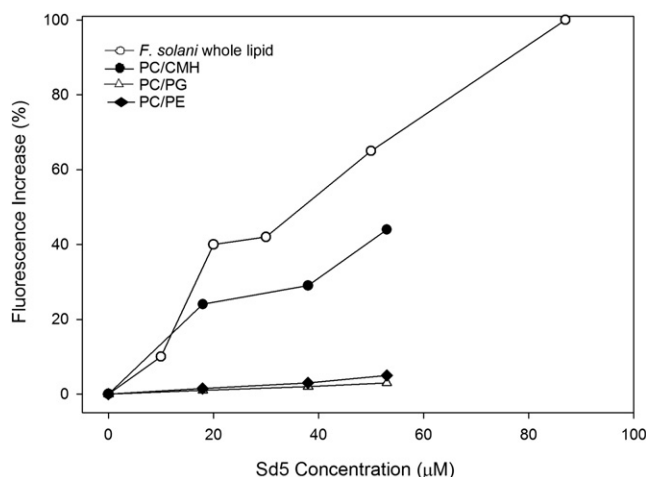


Figure 6. Fractional ANTS Fluorescence Increase Caused by Leakage from LUVs as a Function of Defensin Concentration

Defensin was added to 400 μM vesicles with entrapped DPX and ANTS at time 0. Fractional fluorescence increase is due to ANTS/DPX leakage. The zero level corresponds to vesicle fluorescence in the absence of defensins and the maximum level of fluorescence, scaled to a value of 100%, is determined by complete lysis of vesicle with Triton X-100. The results show that Sd5 induces leakage of *F. solani* lipid and PC/CMH vesicles.

See also Table S3.

different mechanisms of interacting with the membrane. Their structures are designed to accommodate mutations as an important tool in avoiding resistance. Usually, only a small number of amino acids are essential for activity (De-Paula et al., 2008). For this reason, a great deal of effort has been expended to understand the structure-function relationships of membrane-destabilizing peptides with the aim of rationally designing novel peptides that are potentially important for biotechnological applications in the fields of antibiotics, biosensors and drug delivery. These relationships among antimicrobial peptides are neither obvious nor easily predictable. Wimley and co-workers described ten peptides selected from a 16,384 member combinatorial library based on their ability to permeabilize synthetic lipid vesicles in vitro (Rathinakumar and Wimley, 2008). In spite of the lack of common sequence motif, the peptides shared a mechanism of action that is similar to membrane permeabilizing AMP. In addition, single D-amino acid substitutions eliminated or diminished the secondary structure of the peptides but they retained activity against some microbes. In human β -defensins the replacement of cysteines by α -aminobutyric acid does not interfere in the antibacterial activity but does change the chemotactic properties of the protein (Wu et al., 2003). Thus, the coupling between the structure and biological activity is not easy to determine. Based on our results, a specific region in the defensins is responsible for activity and other regions are important for the destabilization of membranes and disturbing the organization of the lipids.

As we showed previously, Sd5 exhibits a recent gain of function, as it shows similarity only within its own tribe (the Andropogoneae). This peptide exhibits broad-spectrum activity against different classes of fungi at micromolar concentrations (De-Paula et al., 2008). In the present study, the three-dimensional structure of Sd5 determined by NMR methods revealed the

standard tertiary fold for a defensin, except for the presence of an unstructured C-terminal region that has not been identified in any plant defensin structure reported in the PDB. The flexible C-terminal region of Sd5 revealed a predominance of hydrophobic residues (i.e., Ala, Gly, Leu, and Trp) as well as charged residues (i.e., Arg, Glu, and Lys) that participate in defensin-membrane interaction. This observation is in agreement with previous findings that basic residues (in particular, arginines) and core hydrophobicity are important for the permeabilization of membranes (Rathinakumar and Wimley, 2008).

Protein function is intrinsically coupled to structural plasticity. Thus, knowledge of the three-dimensional structure and dynamical behavior is crucial for understanding the process that requires transient population of excited conformational states, such as molecular recognition by conformational selection (Tsai et al., 1999; Henzler-Wildman and Kern., 2007; Volkman et al., 2001; Valente et al., 2006; Frauenfelder et al., 1988; James and Tawfik, 2003; Cserehely et al., 2010). In this study, we characterized the backbone conformational dynamics of Sd5 using ^{15}N spin relaxation measurements. The dynamic properties of Sd5 are completely different from those of Psd1, a pea defensin (de Medeiros et al., 2010). This is the first dynamic characterization, to our knowledge, that shows several regions in the protein with heterogeneous R_2 values, that is, testing large conformational exchange fluctuations on the μs -ms timescale.

Recent studies have demonstrated that protein dynamics are crucial for signal transduction (Smock and Gierasch, 2009) and can even play an important role in evolution (Tokuriki and Tawfik, 2009). Although for many proteins it is not yet understood how their movements can affect their function and how their dynamics can be related to their three-dimensional fold, there is a link between dynamics and the conformational variability explored within a family of homologous proteins (Friedland et al., 2009; Law et al., 2009).

Using ^{15}N CPMG relaxation dispersion NMR experiments we characterized motions on the ms timescale in Sd5. At least two distinct processes were observed, revealing k_{ex} values of 490 and 1800 s^{-1} . Notably, these processes involve sets of residues that are located in loop 1, part of the α helix, strands $\beta 1$ and $\beta 3$ and in the specific binding site as monitored by chemical shift perturbation (Figure 4). It is probable that the mechanisms of conformational exchange observed in Sd5 involve a transient twisting or “breathing” of the β sheet and α helix. We speculate that changes in the N-H[...] $\text{O}=\text{C}$ hydrogen bond distances might be related to the amplitudes of the conformational fluctuations observed here. Some evidences of slow collective motions across hydrogen-bond networks have been reported for protein G based on residual dipolar couplings and hydrogen bond scalar couplings. The authors found that the protein reveals a heterogeneous distribution of slow dynamics that occur in the loops and β sheet and that the motion is correlated and propagated through interstrand hydrogen bonds (Bouvignies et al., 2005).

Although different methods will be needed to fully clarify the complex nature of the motions undergone by Sd5, the importance of dynamic properties and binding events has long been recognized. Freire (1999) pointed out that, in biological systems, binding event occurs through multiple events involving high and low structural stability residues. If the binding site were formed

by high stability residues only, the binding would induce only an energy shift. On the other hand, the presence of low-structural stability residues permits redistribution in the conformational ensemble and a propagation of the effect to regions far from the binding site. The stabilized state will have desired set of functional features. Upon membrane binding Sd5 needs to change from a soluble and stable protein to an “interacting state.” To complete its biological function, Sd5 must interact with its cellular targets.

Furthermore, our results showed that Sd5 complex dynamic behavior changes upon membrane interaction. In the early stages, Sd5 probed the surface, exhibiting an increase in exchange on the μs -ms timescale both in the interacting and contiguous regions. The membrane target, CMH, was perceived during the interaction process. Upon insertion into the hydrophobic core, the protein experienced structure stabilization into several discrete conformers that interconvert slowly. There are several proposed mechanisms for membrane destabilization that include pore or carpet formation and more recently, the phase boundary defects that result from lipid clustering in the presence of antimicrobial agents (Epand and Epand, 2009).

Our findings showed that Sd5 was able to bind to membranes causing permeation that was dependent on CMH. Membrane permeabilization is dependent on a peptide having the correct balance of hydrophobicity, solubility, amphipathicity, and perhaps propensity to self-assemble on membranes into peptide-rich domains (Rathinakumar et al., 2009). We suggest that the leakage from vesicles induced by Sd5 is dependent on a motif that comprises aromatic residues at the lipid-exposed interfacial positions and charged residues at the pore-lining positions. Additionally, we speculate that the side-chains of S34, S36, and Y37 present in the specific binding site (Figure 4C) may interact with the glycosyl part of CMH. A similar result was observed for Psd1 in the presence of DPC:CMH micelles. For Psd1 we found that the aromatic δ protons of Phe 15 show NOEs with the ceramide part of CMH and that the β protons of Thr16 show several unambiguous NOEs with the glycosyl part of CMH (de Medeiros et al., 2010).

Other interesting feature for this defensin is shown in Figure S7, for selected residues in the presence of different concentrations of DPC micelles. Note that the number of conformers increases in the presence of 60 mM DPC when compared to Sd5 free in solution, however in the presence of 300 mM DPC a small number of conformers is again stabilized, but these were different from the conformation in solution. Further experiments will completely elucidate this process.

In summary, attributes such as specificity and affinity can be explained by characterization of the dynamic properties of interaction surfaces. Here, we showed that interactions with interfaces cause proteins to exhibit complex dynamic properties that depend on the stage of interaction. In the early stages, there is an increase in protein dynamics. In the later stages, there is an increase in order that may be compensated for by a decrease in membrane organization that leads to disruption. The structural fluctuations observed here suggest a structural plasticity that may prove significant for interactions with lipid membranes and its various cellular receptors.

This suggests that conformational selection may be the mechanism of Sd5-membrane interaction. Instead of being folded into

a single native conformation, proteins have evolved to sample multiple defined conformations that are essential for function (Tsai et al., 1999). The amino acids responsible for creating the plasticity are probably the ones conserved during evolution and are not necessarily direct responsible for biological activity (Friedland et al., 2009).

In conclusion, there are few studies of the dynamical properties of defensins: Sd5, in the present manuscript and Psd1, another study by our group (de Medeiros et al., 2010). These studies show that although the structures are similar, the dynamics are remarkably different. We are showing that the dynamics provides ways of understanding mechanisms and mapping binding sites of defensins and other proteins that bind transiently to the membrane. The conformational selection is playing important role in membrane recognition. Conformations that are pre-existent in the free state of the defensins are important for recognition of CMH at the membrane interface.

EXPERIMENTAL PROCEDURES

Protein Sample Preparation

Sd5 was overexpressed in *Escherichia coli* strain BL21(DE3) as a N-His₆ fusion protein and purified as recently described (De-Paula et al., 2008). The sample used for NMR spectroscopy was 0.2–1.0 mM Sd5 in 5 mM sodium phosphate buffer (pH 4.0), containing 10% D₂O, and 5 mM sodium azide. Additional methods are described in the Supplemental Experimental Procedures.

Structure Calculation

NMR spectra were recorded using ¹⁵N- or ¹³C- labeled samples for Sd5 on a Bruker Avance III 800 MHz spectrometer. All experiments were performed at 25°C. The protein backbone resonance assignments were achieved through analysis of the standard triple resonance experiments. ¹⁵N-edited TOCSY-HSQC acquired with 60 ms spin-lock time was used to resolve ambiguity due to the spectral overlap. The aromatic side chains were assigned using ¹³C-edited NOESY-HSQC aromatic (mixing time of 120 ms) and ¹³C-HMQC experiments. Asparagine and Glutamine side-chain amide protons were stereo-specifically assigned from a ¹⁵N-edited NOESY-HSQC (mixing time of 120 ms) experiment. *Phi* and *psi* torsion angle restraints were predicted based on analysis of ¹HN, ¹⁵N, ¹H_α, ¹³C_α, ¹³CO, and ¹³C_β chemical shifts using the program TALOS (Cornilescu et al., 1999). All NMR data were processed using Topspin 2.0 and analyzed by CARRA version 1.8.4 (Keller and Wuthrich, 2004). The NOE distance restraints were based on a 3D simultaneous ¹³C-edited NOESY-HSQC and ¹⁵N-edited NOESY-HSQC experiment. Semiautomated NOE cross-peak assignments were performed by using the UNIO'10 module (Volk et al., 2008; Fiorito et al., 2008; Herrmann et al., 2002). Structure calculation was carried out using a simulated annealing protocol with torsion angle molecular dynamics with CYANA version 2.1 (Gunter et al., 1997). Additional informations are described in the Supplemental Experimental Procedures. Both the chemical shifts and coordinates of the Sd5 were deposited in the BioMagResBank (BMRB: 16666) and the Protein Data Bank (PDB ID: 2KSK), respectively.

Backbone Dynamics

The relaxation experiments were performed using a Bruker DRX-600 MHz or Bruker Avance III 800 MHz at 15°C, 25°C, and 30°C as detailed in Supplemental Experimental Procedures. The chemical exchange contribution of the transverse relaxation rate of ¹⁵N spins was determined from a set of CPMG relaxation dispersion spectra recorded at 600 and 800 MHz at 25°C, as described in previous studies (Tollinger et al., 2001). See Supplemental Experimental Procedures for all backbone dynamics details.

Vesicle Preparation

Large unilamellar vesicles (LUV, 100 nm in diameter) were prepared according to the extrusion method as detailed elsewhere (de Medeiros et al., 2010). The final concentration of PC or PC:CMH was 5 mM. NMR spectra were recorded

on 200 μM ¹⁵N-labeled Sd5 in 5 mM sodium phosphate buffer (pH 4.0), in the presence or absence of 5 mM PC or PC:CMH (9:1 molar ratio) vesicles. The scaled chemical shift changes ($\Delta\delta$) were calculated using the following equation: $\Delta\delta = (\Delta\omega_H^2 + \Delta\omega_N^2/6.49)^{1/2}$, where $\Delta\omega_H$ and $\Delta\omega_N$ are the chemical shift changes in the presence of vesicles for the ¹H and ¹⁵N dimensions, respectively.

Vesicle Leakage Assay

LUVs of approximately 100 nm in diameter were prepared by the freeze/thaw and extrusion method as previously described (Ladokhin et al., 1997; Takeuchi et al., 2004). Lipid films were resuspended in 10 mM MES, 50 mM KCl, 1 mM EDTA, 9 mM ANTS, 25 mM DPX (pH 6.0). External fluorophores were removed by gel filtration leaving a solution of vesicles with entrapped markers. Vesicles containing ANTS/DPX at about 400 μM were placed into a 1 × 0.2 cm quartz cuvette (volume, 0.5 ml), and the fluorescence increase due to leakage and subsequent dilution of quenched dye was measured after the addition of defensin. Data are presented in terms of fractional fluorescence $fF = (F - F_{\text{initial}})/(F_{\text{max}} - F_{\text{initial}})$, where F is the measured fluorescence, F_{initial} is the initial quenched fluorescence, and F_{max} is the fluorescence corresponding to 100% leakage as established by the addition of 0.4% Triton X-100.

NMR Titrations with Micelles

A set of ¹H-¹⁵N HSQC spectra were recorded (at 600 MHz) using ¹⁵N-labeled Sd5 (concentration, 200 μM) in the presence of 5, 10, 15, 30, and 60 mM DPC (monomer concentration- final protein-to-DPC ratio of 1:50, 1:75, 1:150, and 1:300). All titrations were carried out in 5 mM sodium phosphate buffer (pH 4.0), 5 mM sodium azide and 10% D₂O, and the chemical shift changes ($\Delta\delta$) were calculated as described above.

ACCESSION NUMBERS

Coordinates have been deposited in the PDB with accession code 2KSK, and chemical shifts were deposited in the BioMagResBank with accession code 16666.

SUPPLEMENTAL INFORMATION

Supplemental Information includes Supplemental Experimental Procedures, seven figures, and three tables and can be found with this article online at doi:10.1016/j.str.2010.11.011.

ACKNOWLEDGMENTS

This research was supported by Grants from Conselho Nacional de Desenvolvimento Científico e Tecnológico (CNPq), ICGEB-Trieste, Fundação de Amparo a Pesquisa do Estado do Rio de Janeiro Carlos Chagas Filho (FAPERJ- Pensa Rio), Coordenação de Aperfeiçoamento de Pessoal de Nível Superior (CAPES) and National Institute of Structural Biology and Bioimaging (INBB). We also thank Fabrício Cruz for technical assistance.

Received: August 17, 2010

Revised: November 16, 2010

Accepted: November 17, 2010

Published: January 11, 2011

REFERENCES

- Aerts, A.M., François, I.E.J.A., Cammue, B.P.A., and Thevissen, K. (2008). The mode of antifungal action of plant, insect and human defensins. *Cell. Mol. Life Sci.* 65, 2069–2079.
- Boehr, D.D. (2009). During transitions proteins make fleeting bonds. *Cell* 139, 1049–1051.
- Bouvignies, G., Bernadó, P., Meier, S., Cho, K., Grzesiek, S., Brüschweiler, R., and Blackledge, M. (2005). Identification of slow correlated motions in proteins using residual dipolar and hydrogen-bond scalar couplings. *Proc. Natl. Acad. Sci. USA* 102, 13885–13890.

- Cavanagh, J., and Akke, M. (2000). May the driving force be with you-whatever it is. *Nat. Struct. Biol.* 7, 11–13.
- Csermely, P., Palotai, R., and Nussinov, R. (2010). Induced fit, conformational selection and independent dynamic segments: an extended view of binding events. *Trends Biochem. Sci.* 35, 539–546.
- Cornilescu, G., Delaglio, F., and Bax, A. (1999). Protein backbone angle restraints from searching a database for chemical shift and sequence homology. *J. Biomol. NMR* 13, 289–302.
- DeLano, W.L. (2002). *The PyMOL User's Manual* (Palo Alto, CA: DeLano Scientific).
- de Medeiros, L.N., Angeli, R., Sarzedas, C.G., Barreto-Bergter, E., Valente, A.P., Kurtenbach, E., and Almeida, F.C. (2010). Backbone dynamics of the antifungal Psd1 pea defensin and its correlation with membrane interaction by NMR spectroscopy. *Biochim. Biophys. Acta* 1798, 105–113.
- De-Paula, V.S., Razzera, G., Medeiros, L., Miyamoto, C.A., Almeida, M.S., Kurtenbach, E., Almeida, F.C., and Valente, A.P. (2008). Evolutionary relationship between defensins in the Poaceae family strengthened by the characterization of new sugarcane defensins. *Plant Mol. Biol.* 68, 321–335.
- Dosset, P., Hus, J.C., Blackledge, M., and Marion, D. (2000). Efficient analysis of macromolecular rotational diffusion from heteronuclear relaxation data. *J. Biomol. NMR* 16, 23–28.
- Epand, R.M., and Epand, R.F. (2009). Domains in bacterial membranes and the action of antimicrobial agents. *Mol. Biosyst.* 5, 580–587.
- Fiorito, F., Damberger, F.F., Herrmann, T., and Wüthrich, K. (2008). Automated amino acid side-chain NMR assignment of proteins using ¹³C- and ¹⁵N-resolved 3D [(1)H, (1)H]-NOESY. *J. Biomol. NMR* 42, 23–33.
- Forman-Kay, J.D. (1999). The “dynamics” in the thermodynamics of binding. *Nat. Struct. Biol.* 6, 1086–1087.
- Frauenfelder, H., Parak, F., and Young, R.D. (1988). Conformational substates in proteins. *Annu. Rev. Biophys. Chem.* 17, 451–479.
- Frederick, K.K., Marlow, M.S., Valentine, K.G., and Wand, A.J. (2007). Conformational entropy in molecular recognition by proteins. *Nature* 448, 325–329.
- Freire, E. (1999). The propagation of binding interactions to remote sites in proteins: analysis of the binding of the monoclonal antibody D1.3 to lysozyme. *Proc. Natl. Acad. Sci. USA* 96, 10118–10122.
- Friedland, G.D., Lakomek, N.A., Griesinger, C., Meiler, J., and Kortemme, T. (2009). A correspondence between solution-state dynamics of an individual protein and the sequence and conformational diversity of its family. *PLoS Comput. Biol.* 5, e1000393.
- Gardino, A.K., Villali, J., Kivenson, A., Lei, M., Liu, C.F., Steindel, P., Eisenmesser, E.Z., Labeikovsky, W., Wolf-Watz, M., Clarkson, M.W., and Kern, D. (2009). Transient non-native hydrogen bonds promote activation of a signaling protein. *Cell* 139, 1109–1118.
- Gunter, P., Mumenthaler, C., and Wüthrich, K. (1997). Torsion angle dynamics for NMR structure calculation with the new program DYANA. *J. Mol. Biol.* 273, 283–298.
- Henzler-Wildman, K., and Kern, D. (2007). Dynamic personalities of proteins. *Nature* 450, 964–972.
- Henzler-Wildman, K.A., Thai, V., Lei, M., Ott, M., Wolf-Watz, M., Fenn, T., Pozharski, E., Wilson, M.A., Petsko, G.A., Karplus, M., et al. (2007). Intrinsic motions along an enzymatic reaction trajectory. *Nature* 450, 838–844.
- Herrmann, T., Günter, P., and Wüthrich, K. (2002). Protein NMR structure determination with automated NOE assignment using the new software CANDID and the torsion angle dynamics algorithm DYANA. *J. Mol. Biol.* 319, 209–227.
- James, L.C., and Tawfik, D.S. (2003). Conformational diversity and protein evolution—a 60-year-old hypothesis revisited. *Trends Biochem. Sci.* 28, 361–368.
- Keller, R., and Wüthrich, K. (2004). Computer-aided resonance assignment (CARA). Available at: <http://www.nmr.ch>.
- Ladokhin, A.S., Wimley, W.C., Hristova, K., and White, S.H. (1997). Mechanism of leakage of contents of membrane vesicles determined by fluorescence quenching. *Methods Enzymol.* 278, 474–486.
- Law, A.B., Fuentes, E.J., and Lee, A.L. (2009). Conservation of side-chain dynamics within a protein family. *J. Am. Chem. Soc.* 131, 6322–6323.
- Lee, A.L., Kinnear, S.A., and Wand, A.J. (2000). Redistribution and loss of side chain entropy upon formation of a calmodulin-peptide complex. *Nat. Struct. Biol.* 7, 72–77.
- Leng, J., Egelhaaf, S.U., and Cates, M.E. (2003). Kinetics of the micelle-to-vesicle transition: aqueous lecithin-bile salt mixtures. *Biophys. J.* 85, 1624–1646.
- Loria, J.P., Berlow, R.B., and Watt, E.D. (2008). Characterization of enzyme motions by solution NMR relaxation dispersion. *Acc. Chem. Res.* 41, 214–221.
- Meiler, J., Prompers, J.J., Peti, W., Griesinger, C., and Brüschweiler, R. (2001). Model-free approach to the dynamic interpretation of residual dipolar couplings in globular proteins. *J. Am. Chem. Soc.* 123, 6098–6107.
- Mittermaier, A.K., and Kay, L.E. (2009). Observing biological dynamics at atomic resolution using NMR. *Trends Biochem. Sci.* 34, 601–611.
- Mulder, F.A., Mittermaier, A., Hon, B., Dahlquist, F.W., and Kay, L.E. (2001). Studying excited states of proteins by NMR spectroscopy. *Nat. Struct. Biol.* 8, 932–935.
- Palmer, A.G. (2004). NMR characterization of the dynamics of biomacromolecules. *Chem. Rev.* 104, 3623–3640.
- Rathinakumar, R., and Wimley, W.C. (2008). Biomolecular engineering by combinatorial design and high-throughput screening: small, soluble peptides that permeabilize membranes. *J. Am. Chem. Soc.* 130, 9849–9858.
- Rathinakumar, R., Walkenhorst, W.F., and Wimley, W.C. (2009). Broad-spectrum antimicrobial peptides by rational combinatorial design and high-throughput screening: the importance of interfacial activity. *J. Am. Chem. Soc.* 131, 7609–7617.
- Smock, R.G., and Gierasch, L.M. (2009). Sending signals dynamically. *Science* 324, 198–203.
- Takeuchi, K., Takahashi, H., Sugai, M., Iwai, H., Kohno, T., Sekimizu, K., Natori, S., and Shimada, I. (2004). Channel-forming membrane permeabilization by an antibacterial protein, sapecin: determination of membrane-buried and oligomerization surfaces by NMR. *J. Biol. Chem.* 279, 4981–4987.
- Thevissen, K., Warnecke, D.C., Francois, I.E., Leipelt, M., Heinz, E., Ott, C., Zahringer, U., Thomma, B.P., Ferket, K.K., and Cammue, B.P. (2004). Defensins from insects and plants interact with fungal glucosylceramides. *J. Biol. Chem.* 279, 3900–3905.
- Tokuriki, N., and Tawfik, D.S. (2009). Protein dynamism and evolvability. *Science* 324, 203–207.
- Tollinger, M., Skrynnikov, N.R., Mulder, F.A., Forman-Kay, J.D., and Kay, L.E. (2001). Slow dynamics in folded and unfolded states of an SH3 domain. *J. Am. Chem. Soc.* 123, 11341–11352.
- Tsai, C.J., Ma, B., and Nussinov, R. (1999). Folding and binding cascades: shifts in energy landscapes. *Proc. Natl. Acad. Sci. USA* 96, 9970–9972.
- Valente, A.P., Miyamoto, C.A., and Almeida, F.C. (2006). *Curr. Med. Chem.* 13, 3697–3703.
- Vallurupalli, P., and Kay, L.E. (2006). Complementarity of ensemble and single-molecule measures of protein motion: a relaxation dispersion NMR study of an enzyme complex. *Proc. Natl. Acad. Sci. USA* 103, 11910–11915.
- Volk, J., Herrmann, T., and Wüthrich, K. (2008). Automated sequence-specific protein NMR assignment using the memetic algorithm MATCH. *J. Biomol. NMR* 41, 127–138.
- Volkman, B.F., Lipson, D., Wemmer, D.E., and Kern, D. (2001). Two-state allosteric behavior in a single-domain signaling protein. *Science* 291, 2429–2433.
- Wolf-Watz, M., Thai, V., Henzler-Wildman, K., Hadjipavlou, G., Eisenmesser, E.Z., and Kern, D. (2004). Linkage between dynamics and catalysis in a thermophilic-mesophilic enzyme pair. *Nat. Struct. Mol. Biol.* 11, 945–949.
- Wu, Z., Hoover, D.M., Yang, D., Boulegue, C., Santamaria, F., Oppenheim, J.J., Lubkowski, J., and Lu, W. (2003). Engineering disulfide bridges to dissect antimicrobial and chemotactic activities of human beta-defensin 3. *Proc. Natl. Acad. Sci. USA* 100, 8880–8885.